

# Electrochemistry Theorem Based State-of-Charge Estimation of the Lead Acid Batteries for Electric Vehicles

YING-SHING SHIAO, DING-TSAIR SU, JUI-LIANG YANG, RONG-WEN HUNG

Department of Electrical Engineering  
National Changhua University of Education  
No. 2 Shi-Da Rd., Changhua City, 500 Taiwan  
REPUBLIC OF CHINA (TAIWAN)  
sdt@ctu.edu.tw, <http://www.ncue.edu.tw>

**Abstract:** - A method for the estimation of the state-of-charge in lead-acid batteries for electric vehicles is investigated. The electrochemistry theorem is introduced to measure the resistance effect of the electrode reaction and to estimate the internal energy loss and the electrolyte specific gravity in batteries. The proposed algorithms can accurately compute the state-of-charge of the lead-acid batteries, that the variations of the electrochemical resistance in the electrolyte concentrations are estimated for the state-of-charge. The approach is based on the idea of constructing the real time approach that can be implemented by a digital signal processor. The motivation of this work is to explore the problem of different procedures on the charged and discharged of the lead-acid batteries to obtain the variations in the charge-discharge and resistance profiles. The provided method shows that it is validated for estimation the capacitances and residue energies.

**Key-Words:** - State-of-charge, Lead-acid battery, Electric vehicles, Electrode reaction, Electrolyte specific gravity, Digital signal processor.

## 1 Introduction

The need to develop electric vehicles (EVs) arises not only due to the high price of international petroleum but also for solving the worsening environment problems. Currently, energy management is the major key technology of battery powered vehicle [1]. The increase of energy density and efficiency, and accurate measurement of the state-of-charge (SOC), etc. are important research topics [2, 3]. Although many new electrochemical systems are under study for this application, the lead acid battery is still a leading candidate [4]. In this paper, the measurement of the SOC of the lead acid battery in battery powered vehicle is studied. The approach for estimating the SOC of the battery uses the electrochemical reaction during the charging or discharging of the lead acid battery.

Generally, the methods for measuring the SOC of the lead acid battery are: impedance method, conductance method or resistance method [5, 6]. These methods have been implemented as instruments for measuring the SOC of the battery in the off-line state. In the previous study, the method was proposed to estimate the SOC of the battery by measuring the AC ripples during the charging state of the battery. However, such approach is not suitable for vehicles that are driving. In the study [7, 8], the method was proposed to use the transient characteristics of the battery during the initial

discharging period to measure the SOC of the batteries in communication systems.

The methods use the relationship of the discharge voltage over time for measuring the SOC of lead acid batteries that can be roughly categorized into two types: one is the parametric-fitting model and the other is the curve-fitting model. In the study [9], the internal resistance of the battery is used for the parametric-fitting model. The characteristic curve of the discharge voltage over time provided by the manufacturer is corrected with the internal resistance to allow the measurement of the SOC of the battery. However, the internal resistance of the battery is not a constant. Thus, such method may not be accurate enough for the measurement of the SOC of the lead acid battery in the EVs. In the studies [10, 11], the parametric-fitting, parabolic-fitting or their combines are used to emulate the characteristic curve of the discharge voltage over time. The disadvantage of such methods is that only the batteries of the same model are used for the discharge test, and the obtained data is then used to construct the discharge curve. If the battery of the same model has some difference, this approach does not work anymore. In order to solve the above mentioned disadvantages, the Coulometric accumulation method that can measure the charge or discharge current of the battery is proposed [12-14]. This method requires the correction factor for the

different discharge rates due to different ambient temperatures. Also, this method strongly relies on the history information of the battery and there will be accumulated errors.

The method that uses the state estimator or the fuzzy theory to estimate the state of the battery was proposed [10]. However, the accuracy of this method can not be improved due to the limitation of the measurement accuracy of the internal resistance because the internal resistance is usually very low and will vary along with the aging of the battery.

Currently, the methods for measuring the SOC of the lead acid battery in industry are as follows: specific gravity method, open circuit voltage method, Coup de Fouet method, loaded voltage method, internal resistance method and Coulometric measurement method [9, 14-16]. Among these methods, the specific gravity method is not economical because it requires an additional specific gravity gauge and it is not suitable for the valve-regulated lead-acid battery (VRLA) [17]. The Coup de Fouet method is suitable only when the battery is fully charged, thus it is applicable for a narrow range. The internal resistance is suitable for off-line systems to detect whether the battery reaches its final phase of the discharge. These methods are not suitable for measuring the SOC of the batteries in the EVs.

For battery-powered motorcycles (BPMs) which use the lead acid battery as its power source, the discharge of the battery is irregular so there is no single method that can precisely measure the SOC of the lead acid battery. Hence, the studies usually adopt the combination of several measurement methods to compensate the disadvantage of each method.

For the open circuit method, loaded voltage method and the Coulometric measurement method, because the measurement targets for the three methods are the same, i.e., the voltage and current of the battery, there is no need for additional circuits to combine with each other. Thus these methods can be combined to measure the SOC of the battery in the battery-powered vehicles [18].

Although the open circuit voltage method is accurate to some extent. In fact, for accurate measurement results of the open circuit voltage, the lead acid battery must be kept in a steady state after being charged or discharged for a while until the concentration of the electrolyte becomes uniform. Thus, the open circuit voltage method is not practical. The Coulometric measurement method integrates the charge coming in or out the battery which is expressed as the Ampere-hour product to represent the charge being added or subtracted. In

this method, the internal loss of the lead acid battery is not considered, thus a relatively large error will be generated. For practical application, the Coulometric measurement method is frequently used to measure the SOC due to its ease of use. Thus in the BPMs, this method is adopted currently for the calculation.

Because the Coulometric measurement method uses the summation method for the calculation, usually there will be several correction factors added to minimize the error and used together to determine the SOC. For example, during the charging period, the terminal voltage is measured, the rising slope of the voltage is measured, or the end of discharge voltage (EODV) is set, etc. for this purpose.

Although the Coulometric measurement method is convenient to use, it still has the following disadvantages: it is based on the measurement of the actual current and rated capacity. In fact, the capacity of the battery depends strongly on the discharge current, thus the estimation will be inaccurate for cases with large discharge current. Because the battery aging effect will also reduce the capacity, if it is not corrected, an error may occur. Thus, some researchers proposed to use the modified Coulometric measurement method which uses the Coulometric measurement method as the basis and considered the current additive effect and the battery aging factor [19].

For the measurement methods for the SOC, the additive effect of the battery capacity due to the discharge current is considered. First, the relationship between the actual current and the additive effect current is depicted. Secondly, these multiplication relationships between the actual current and the additive effect current are studied. Finally, the minimum square method is used to calculate the multiplication curve to estimate the SOC of the battery. Thus, the obtained SOC measurement can be accurate enough to some extent.

As for considering the battery aging factor and the correction of its capacity, the correction of the SOC is determined by using the slope of the voltage over time during the battery discharge. During the initial period of the discharge, the voltage of each battery is approximately the same. While more than 70% of the capacity is being discharged, the voltage of the severely old battery will decrease drastically. Thus, such property can be used to correct the SOC of the old battery [18-20].

As mentioned above, the reaction of the electrode of the battery is strongly and directly related to the SOC. In this paper, the proposed measurement method of the SOC of the lead acid battery is to use the basic theory of electrochemistry to determine the electrochemical reaction parameters related to the

SOC. The first electrochemical effective circuit for the reaction of the electrode was proposed since 1899 by Warburg, who proposed the diffusion controlled reactive impedance for plate electrodes, which is now known as Warburg impedance. The research in recent years emphasizes the electrodynamics of the charge transfer reaction [19, 21]. These effects are the important factors that cause the conversion of chemical energy into electrical energy. In this paper, the electrochemical theory for these reactions of the electrode is used to calculate the chemical parameters for the electrode reaction and the circuit is also designed to calculate the variation of the electrochemical parameters of the battery to measure the SOC of the lead acid battery.

## 2 Algorithms for the SOC of Lead Acid Battery

When the battery is loaded, the reaction of the electrode will cause the internal loss of the battery due to the direct connection between the electrode reaction and the current of the load. Thus, with this approach, the additive effect due to the battery aging and discharge current can be obtained. Then the electrochemical theory is used to calculate the resistance effect by the electrode reaction to estimate the internal loss of the battery. As a result, the SOC of the battery can be accurately calculated in real time.

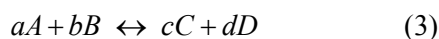
The battery is an electrochemical device which can convert the chemical energy into electrical energy by the oxidation reduction reaction (redox) of the electrodes. The reduction reaction of one of the battery electrodes can be expressed generally in the following expression:



where atom  $A$  of the number of  $a$  and  $n$  electrons react to form atom  $C$  of the number of  $c$ . In the same way, the oxidation reaction of the other electrode can be expressed as (2) :

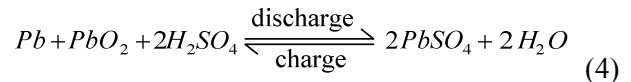


where atom  $B$  of the number of  $b$  and  $n$  electrons react to form atom  $D$  of the number of  $d$ . The entire reactions of the battery are the summation of the above two reaction of the half-cell as follows:



with these expressions, the redox reaction of the electrodes of the lead acid battery can be expressed in the following expression:

Overall reaction:



The chemical energy of the battery is converted into the maximum electrical energy output, which can be expressed by  $\Delta G$ , the standard free energy of the reaction of the electrode:

$$\Delta G = -nFE^0 \quad (5)$$

where  $F$  is the Faraday constant (96,487C) and  $E^0$  is the standard electromotive force (emf) of the battery. While in state different from the standard, the voltage of the battery can be expressed by Nernst Equation as follows [21]:

$$E = E^0 - \frac{GT}{nF} \ln \frac{a_c^c a_D^d}{a_A^a a_B^b} \quad (6)$$

where  $G$  in (6) is the gas constant,  $T$  is the temperature of the battery and  $a_i^i$  is the reactants of the electrodes. The Nernst Equation of a lead acid battery can be expressed as follows:

$$E = E^0 - \frac{GT}{nF} \ln \frac{H_2SO_4}{H_2O} \quad (7)$$

Usually,  $\Delta G$  is expected to be fully converted into electrical energy during discharge. However, when the current  $I$  is extracted and flowing through the battery, the accompanied electrochemical reaction along with the electrode will cause activation polarization and concentration polarization. Meanwhile, the electrolyte may exhibit a resistance of  $R_{bi}$ , which may dissipate a part of the energy  $\Delta G$ . Hence, when the battery is connected with an external load  $R$ , the terminal voltage of the battery can be expressed as follows:

$$E = E^0 - [(\eta_{ap})_a + (\eta_{cp})_a] - [(\eta_{ap})_c + (\eta_{cp})_c] - IR_t = IR \quad (8)$$

where  $(\eta_{ap})_a$  and  $(\eta_{ap})_c$  are the activation polarization of the anode respectively, and cathode,  $(\eta_{cp})_a$  and  $(\eta_{cp})_c$  are the concentration polarization of the anode and cathode respectively. These polarization effects can be expressed by Tafel Equation [21]:

$$\eta = a \pm b \log i \quad (9)$$

where  $\eta$  equals to  $E - E^0$ ,  $a$  and  $b$  are constant. If  $\eta$  represents the vertical axis and  $\log i$  represents the horizontal axis, the slope  $b$  is called Tafel Slope. The above expression can be rearranged in logarithmic form as follows:

$$i = \exp(\pm \frac{a}{b}) \exp \frac{\eta}{b} \quad (10)$$

where  $aA$  in (1) represents the oxidized agent (such as  $Pb^{2+}$ ) and  $C$  represents the reduced agent (such as  $Pb$ ). If the forward and reverse reaction constants

are represented by  $K_f$  and  $K_b$  respectively, and the reaction rate can be expressed as the product of the reaction constant and the concentration of the related reactants. By applying the mass reaction theory on the forward reaction and reverse reaction on the surface of the electrodes, the reaction rates can be expressed by the forward current  $i_f$  and the reverse current  $i_b$  as follows:

$$i_f = nAFK_f C_O \quad (11)$$

$$i_b = nAFK_b C_R \quad (12)$$

where  $C_O$  and  $C_R$  represent the concentrations of the oxidation agent and reduction agent respectively, and  $A$  is the surface area of the electrode. The electron in the reaction is influenced by the electric potential of the electrode. For the forward (reverse) reaction, it can be expressed as  $\alpha E$  and  $(1-\alpha)E$ .  $\alpha$  is called as the transfer factor or the symmetry factor,  $E$  is the electrical potential of the electrode. Thus, due to the effect of the electrical potential of the electrodes, the reaction constants for the forward and reverse are:

$$K_f = K_f^0 \exp \frac{-\alpha nFE}{GT} \quad (13)$$

$$K_b = K_b^0 \exp \frac{(1-\alpha)nFE}{GT} \quad (14)$$

Because in the balance state, there is no net current generated, thus

$$i_f = i_b = i_0 \quad (15)$$

$i_0$  is called as the exchange current. The exchange current is used to express the exchange rate of the charge in the balance state. From (13)-(14), together with (15), the following relationship can be obtained:

$$C_O K_f^0 \exp \frac{-\alpha nFE_e}{GT} = C_R K_b^0 \exp \frac{(1-\alpha)nFE_e}{GT} \quad (16)$$

where  $E_e$  is the electric potential in balance. The above expression can be rearranged as follows:

$$E_e = \frac{GT}{nF} \ln \frac{K_f^0}{K_b^0} + \frac{GT}{nF} \ln \frac{C_O}{C_R} \quad (17)$$

$$E_e = E^0 + \frac{GT}{nF} \ln \frac{C_O}{C_R} \quad (18)$$

where  $E^0 = \frac{GT}{nF} \ln \frac{K_f^0}{K_b^0}$  is the standard electromotive force. Eq. (18) can be used to express the Nernst Equation, which is similar to (6). The major difference is that (18) is expressed with the concentrations of the reactants in the lead acid battery, where  $C_O$  represents the concentration of  $H_2SO_4$ , and  $C_R$  represents the concentration of  $H_2O$ .

From (11) and (12) under the balance condition, we can obtain:

$$i_o = i_f = nFAC_O K_f^0 \exp \frac{-\alpha nFE_e}{GT} \quad (19)$$

by combining with (11), (13), (17) and (19), it can be rearranged as:

$$i_o = nFAC_O^{(1-\alpha)} K_f^{0(1-\alpha)} K_b^{0\alpha} C_R^\alpha = nFAKC_O^{(1-\alpha)} C_R^\alpha \quad (20)$$

where  $K = K_f^{0(1-\alpha)} K_b^{0\alpha}$ .

The effect of the reaction of the electrodes is described by (20). When the unbalance occurs, the electric potential of the electrode varies and causes the current of the electrode to tend to the forward current  $i_f$  or the reverse current  $i_b$ , where the direction of the current of the electrode depends on the variation of the direction of the electric potential  $E$ . If the current of the electrode is  $I$ , the voltage on the electrode is  $E = E_e + E'$ , from (11) and (13),  $i_f$  can be expressed by  $i'_f$  as follows:

$$I = i'_f = nFAC_O K_f^0 \exp \frac{-\alpha nF(E_e + E')}{GT} \quad (21)$$

where  $E'$  is the increased electric potential in the unbalance state. By comparing with (19), we can obtain:

$$I = i_o \exp \frac{-\alpha nFE'}{GT} = i_o \exp \frac{-\alpha nF\eta}{GT} \quad (22)$$

where  $\eta = E - E_e$ . Eq. (22) can be rearranged as:

$$\eta = \frac{GT}{\alpha nF} \ln i_o - \frac{GT}{\alpha nF} \ln I \quad (23)$$

This equation has the same meaning as the Tafel Equation expressed in (9).

With the above analysis, when the unbalance occurs, we can obtain the net current  $I$  flowing in or out of the battery, i.e.:

$$I = i_f - i_b \quad (24)$$

By the substitution for (11)-(14) and (18), we can obtain:

$$I = nFAK \left[ C_O \exp \frac{-\alpha nFE^0}{GT} - C_R \exp \frac{(1-\alpha)nFE^0}{GT} \right] \quad (25)$$

where the electrochemical parameters (except  $C_O$ ,  $C_R$  and  $T$  are variables) can be regarded as constants. Thus (25) can be simplified as:

$$I = M [C_O \exp(BT^{-1}) - C_R \exp(CT^{-1})] \quad (26)$$

where  $M = nFAK$ ,  $B = -\alpha nFE^0 G^{-1}$ ,  $C = (1-\alpha)nFE^0 G^{-1}$ . If the temperature effect is neglected, i.e.,  $T$  is regarded as a constant, (26) can be further simplified as:

$$I = \overline{M} C_O - \overline{M} C_R \quad (27)$$

where  $\overline{M} = M \exp(BT^{-1})$ ,  $\overline{M} = M \exp(CT^{-1})$ .

If the resistance of the electrolyte  $R_{bi}$  can be measured in the off-line state, and the current  $I$  in (8) of the battery with an external load can be measured, the terminal voltage of the electricity supplying battery in (8) can be rearranged as:

$$E + IR_{bi} = E^0 - [(n_{ap})_a + (n_{cp})_a] - [(n_{ap})_c + (n_{cp})_c] = E^0 - IR_{EP} \quad (28)$$

where  $R_{EP}$  represents the impedance generated by the reaction of the electrode. By comparing with (20), we can obtain:

$$-IR_{EP} = \frac{GT}{nF} \ln \frac{C_O}{C_R} \quad (29)$$

Because we can measure  $IR_{EP}$  from (28), by substituting for (29), we can obtain the ratio of  $C_O$  to  $C_R$ , and then substitute the value for (25), and then the values of  $C_O$  and  $C_R$  can be obtained. As a result, we can design electric circuits to implement (25)-(29). After obtaining the values of  $C_O$  and  $C_R$ , the SOC of the battery can be obtained.

### 3 Verification Method

In this paper, we use the electrochemical theory to calculate the resistance effect generated by the reactions of the electrodes and then use them to estimate the concentration of the electrolyte inside the battery to measure the variation of the SOC of the battery in the BPM which is moving in the constant speed mode or in the driving mode. In the experiment, the battery in the BPM is fully charged (the voltage is approximately 52.4V for the new battery and 49.58V for the old battery). The BPM is controlled in the constant speed mode and the acceleration/deceleration driving mode to measure the SOC until the discharge voltage decreases to become 42.9V. The measured voltage and current of the battery during the experiment are then put into (28) for the calculation to obtain  $R_{EP}$ . Then,  $R_{EP}$  is used in (29) to obtain the  $C_O/C_R$  ratio. After the ratio is obtained, it is then put into (30) which is rearranged from (25) to obtain  $C_R$ . Finally,  $C_R$  is then put in (29) to obtain the value of  $C_O$ . All the constants required for the calculation are listed in Table 1.

$$C_R = \frac{I}{nFAK \left[ \frac{C_O}{C_R} \exp \frac{-anFE^0}{GT} - \exp \frac{(1-\alpha)nFE^0}{GT} \right]} \quad (30)$$

The measured concentration of the sulfuric acid can be used to determine the specific gravity of the electrolyte according to the relation between the sulfuric acid and the specific gravity. Then the relation between the specific gravity and the SOC can be used to obtain the SOC of the battery. Fig. 1 shows the relation between the concentration and

the specific gravity. The relation between the specific gravity (SG) and the SOC are listed in Table 2.

Take out the battery from the BPM to perform the off-board and on-board measurements to understand the practicality and the accuracy of the above mentioned method. In order to verify the measurement result of the SOC of the lead acid battery, another two separate measurement method for the SOC are used to compare with the method proposed in this paper. Finally, with the analysis of the experiment results, it is confirmed that the method studied in this paper can improve the accuracy of the measurement of the SOC of the lead acid battery.

Table 1 The parameters for measuring the SOC

$E_0(k_g \cdot m^2 / A \cdot s^3)$	48
$R_{bi}(k_g \cdot m^2 \cdot A^2 \cdot s^2)$	$7.8 \times 10^3$
$F(A \cdot s)$	96487
$G(J / Mol \cdot K)$	8.314
$T(K)$	298.15
$A(m^2)$	0.012
$K$	0.02
$\alpha$	0.5

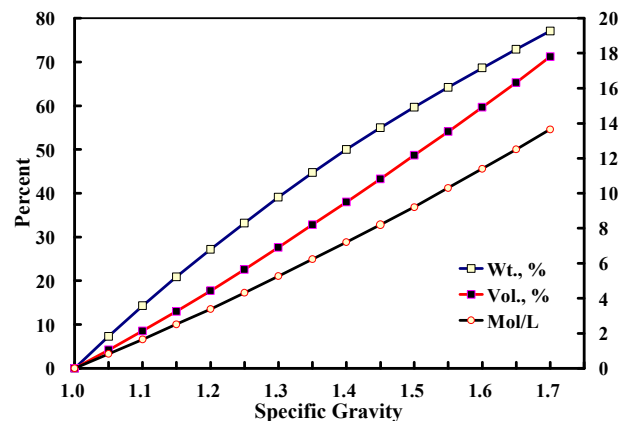


Fig. 1 The relation between the concentration of the sulfuric acid, volume ratio, weight ratio and the specific gravity

Table 2 The relation between the SG and the SOC

SOC	SG
100%	1.330
75%	1.300
50%	1.270
25%	1.240
0%	1.210

The result of the discharge experiment is shown in Fig. 2. The experiment uses the electron load to control the discharge current and the voltage and

current of the battery are separately input into the A/D converter; after calculated by the program, the values of  $C_O$  and  $C_R$  are output from the D/A converter, and the variation of the values of  $C_O$  and  $C_R$  are recorded by the transient recorder.

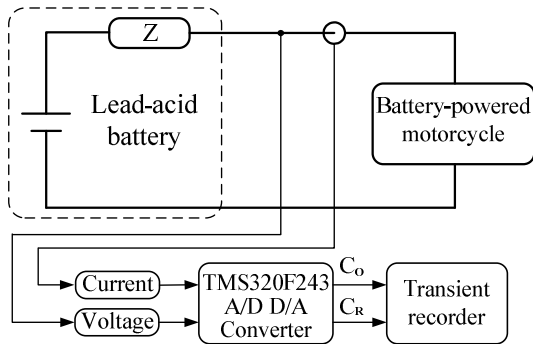


Fig. 2 The setup of the discharge experiment

In order to verify the performance of the lead acid battery under the on-board condition, the BPM is tested on the test platform with various driving speeds, and different driving modes to measure the SOC of the lead acid battery [22]. In the experiment, the BPM is powered by installing the new and old batteries for the experiment respectively. The test procedure is listed in Fig. 3. In Fig. 3, the constant speed test is performed after the battery is fully charged and the BPM is controlled to drive at a constant speed until the battery voltage decreases to the EODV. The driving mode test is performed after the battery is fully charged and the BPM is controlled with the driving cycle shown in Fig. 4 until the battery voltage decreases to the EODV.

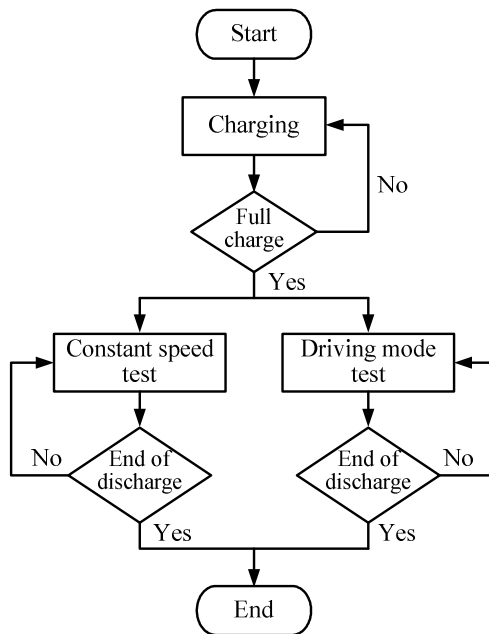


Fig. 3 The flowchart of on-board test of the SOC

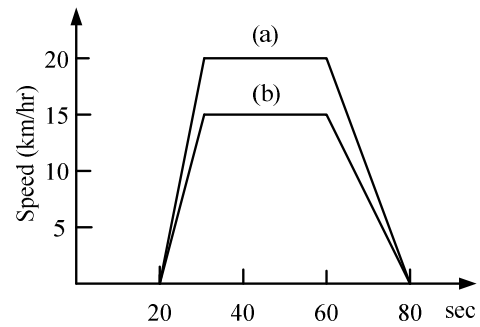


Fig. 4 The driving mode

### 4 Experiment Results

The discharge experiment records the variations of the values of  $C_O$  and  $C_R$  in the transient recorder. In order to verify the measurement of the SOC of the lead acid battery, another two measurement methods for the SOC are used for the comparison with the method proposed in this paper. In Table 3, the first column (a) in the remaining capacity is the experiment result measured with the method proposed in this paper, the second column (b) is the result measured with the open circuit voltage method and the third column (c) is the result measured with the Coulometric measurement method. The open circuit voltage method is performed after the battery is fully discharged and kept for a period of time for the voltage to become in a steady state, the voltage between the two terminals is measured. The advantage of using the open circuit voltage method is that it is quite accurate for the measurement of the SOC. However, the disadvantage is that it needs to keep the battery for a period of time. The requirement of the real time measurement can not be satisfied.

By comparing the results of the method proposed in this paper and the open circuit voltage method, the percentage error of 1.11% and 1.33% in the table might be caused by the experimental error. Most of the remaining errors are within the range of 0.3%-0.4%. It is obvious that the method proposed in this paper can achieve a considerable accuracy.

While testing the BPM on the test platform for the constant speed test with various driving speeds, or for the test with different driving modes, to measure the SOC of the battery. The battery-powered motorcycle is then powered by installing the new and old battery for the test. The test procedure is shown in Fig. 3. After the battery is fully charged, the BPM is controlled to drive at a constant speed. The SOC is then measured until the battery voltage decrease to become the EODV. Another test procedure is performed after the battery

is fully charged. The BPM is controlled in the driving mode shown in Fig. 4. During the driving period, the SOC is measured until it decreases to become the EODV. In order to understand the difference of the power consumption between the constant speed mode and the driving mode, the speed of the driving speed during the constant speed period in the driving mode is controlled the same as the speed in the constant speed mode.

After installing the old battery in the BPM, the constant speed tests of 15km/hr and 20km/hr are performed. During the process of the test, the battery voltage and current are recorded separately as shown in Fig. 5(a) and 5(b). The calculated concentration of the sulfuric acid is shown in Fig. 5(c). From Fig. 5(a), the values of the battery voltage before and after the driving process are 50.1V and 42.9V respectively. Fig. 5(c) shows that the concentration of the sulfuric acid is 5.85Mol/L when the battery is fully charged, after the process where the motorcycle starts driving until it reaches the EODV, the concentration of the sulfuric acid decreases to 3.71Mol/L. According to the relation between the concentration of the sulfuric acid, volume ratio, weight ratio and specific gravity shown in Fig.1, by interpolation, the specific gravities for the concentration of 5.85Mol/L and 3.71Mol/L are 1.316 and 1.217 respectively. After the specific gravity is obtained, by reference to Table 2 the SOC is 88.73% and 5.83% respectively under the constant driving speed of 20km/hr.

After the BPM is installed with the new fully charged battery, the test starts to be performed. All the test procedures are the same as those for the old battery. The constant driving speed tests of 15km/hr and 20km/hr are performed respectively. At 15km/hr, the motorcycle can maintain driving for 23161.37 sec. At 20km/hr, the motorcycle can maintain driving for 12337.32 sec. The test waveform of the new battery under the constant driving speed of 20km/hr is shown in Fig. 6. For the BPM starting with the fully charged battery till stopping due to running out of electricity, the concentrations of the sulfuric acid are 6.08Mol/L and 3.59Mol/L respectively. By using the similar method, the values of the specific gravity of the fully charged and discharged batteries are 1.342 and 1.204 respectively with the concentration of the sulfuric acid  $C_o$  calculated in Fig. 1 and the interpolation method. After the values of the specific gravity are obtained, the SOC before and after driving are 100% and 83% respectively by referring to Fig. 2. Before driving, the SOC of the new battery is 100%, and the internal loss of the battery is smaller. While it reaches the EODV, the

SOC values of the new and old batteries are 0.83% and 5.83% respectively. It shows that the internal loss of the new battery is smaller indeed.

The test results for the constant speed driving are listed in Table 4. According to the analysis of the SOC in the table, the depth of the discharge of the battery installed in the motorcycle with a faster driving speed and the SOC is less. Even new and old batteries are configured with the same EODV, due to the larger internal resistance in the old battery, the SOC after driving is larger. According to the analysis of the above results, no matter if the battery is new or old, or driving under different speeds, correct results can be obtained.

If an old battery is installed in the BPM, the voltage after being fully charged is approximately 50.1V. When it is tested with the mode (a) in Fig. 4, there are total 38 driving cycles. The recorded battery voltage and current are shown in Fig. 7(b) and (c) respectively. The calculated concentration of the sulfuric acid is shown in Fig. 7(d). If the vertical axis (y-axis) in Fig. 7(d) is scaled up, it can be used to calculate the concentration of the sulfuric acid at that moment while the BPM stops after each driving cycle. From Fig. 7(d), it can be shown that the concentration of the sulfuric acid decreases with the driving distance and time of the BPM. Fig. 7(e) shows that the concentration of the sulfuric acid is 5.72Mol/L when the battery is fully charged and the motorcycle starts driving. While the battery is fully discharged, the concentration of the sulfuric acid is 3.67Mol/L. By using the interpolation method for the curve in Fig. 1, the values of the specific gravity are 1.324 and 1.215 respectively for the concentration of 5.72Mol/L and 3.67Mol/L. After the specific gravity is obtained, then the values of the SOC before and after driving are 94.76% and 4.35% respectively by referring to Table 2.

After the BPM is installed with the new battery which is fully charged to be approximately 52.3V, the test is performed in the same way as that for the battery. As the result shown in mode (a) of the Fig. 4, there are total 269 cycles, the recorded data are shown in Fig. 8. When the BPM battery starts driving after being fully charged till it stops after being fully discharged, the concentrations of the sulfuric acid are 6.08Mol/L and 3.58Mol/L respectively and the calculated concentration of is shown Fig. 8(d). In order to record the data for the entire travel, the sampling period is set as  $10^{-8}$  sec per sample. Because the driving time is long, the data points are dense in Fig. 8. In the same way, after the value of  $C_o$  is obtained, the values of the specific gravity after the battery is fully charged and fully discharged are 1.342 and 1.2103 respectively

by interpolation. After the specific gravity is determined and mapped to Table 2, the SOC after being fully charged and discharged are 100% and 0.2% respectively.

The above test results are summarized and shown in Table 5. Comparing the test results in Table 4 and Table 5, the battery has time to rest for the BPM in driving mode, so its travel distance is longer. According to the test results in Table 4 and Table 5, no matter the battery-powered motorcycle is driving at the constant speed mode or in the driving mode, the approach proposed in this paper can be used to accurately measure the SOC of the battery.

## 5 Conclusion

Nowadays, there are several methods that can be used to measure the SOC of lead acid batteries. However, most of them are not suitable for measuring the SOC of the battery in the battery-powered motorcycle due to the irregular discharge characteristic of the battery in a moving vehicle.

In this paper, we propose a measurement method for measuring the SOC of the lead acid battery by using the theory of electrochemical reactions. It can be used to accurately calculate the concentration of the electrolyte inside the lead acid battery in real time, and thus the SOC of the lead acid battery can be obtained. The on board test is performed by placing the battery-powered motorcycle on the test platform. Finally, by means of the test, the measured SOC in the lead acid battery both in on board and off board has a very high accuracy. The test result has verified that the method proposed in this paper can indeed be used to measure the SOC of the battery in the battery in the moving vehicle compared with the battery on board. The measurement of the SOC of the battery, together with the calculation of the power consumption, can be used to estimate the travel range. It can also be used to advise the best driving speed with the knowledge of the driving efficiency of the vehicle to achieve the target of energy management.

### References:

- [1] N. Jinrui, S. Fengchun, and R. Qinglian, A Study of Energy Management System of Electric Vehicles, *IEEE Vehicle Power and Propulsion Conference*, Sep. 2006, pp. 1-6.
- [2] Y. P. Yang and T. H. Hu, A New Energy Management System of Directly-Driven Electric Vehicle with Electronic Gearshift and Regenerative Braking, *American Control Conference, ACC '07*, Jul. 2007, pp. 4419-4424.
- [3] G. Livint, V. Horga, M. Albu, and M. Ratoi, Testing Possibilities of Control Algorithms for Hybrid Electric Vehicles, *The 2nd WSEAS International Conference on Dynamical Systems and Control*, Oct. 2006, pp. 47-52.
- [4] S. Mischie and L. Toma, Behavior of the Lead Acid Battery after the Rest Period, *WSEAS Trans. on Power Systems*, Vol. 3, Issue 3, Mar. 2008, pp. 111-117.
- [5] F. Lacressonniere, B. Cassoret, and J. Brudny, Influence of a Charging Current with a Sinusoidal Perturbation on the Performance of a Lead Acid Battery, *IEE Proceedings on Electric Power Applications*, Vol. 152, Issue 5, Sep. 2005, pp. 1365-1370.
- [6] R. S. Robinson, System Noise as a Signal Source for Impedance Measurement on Batteries Connected to Operating Equipment, *Journal of Power Source*, Vol. 42, 1993, pp. 381-388.
- [7] H. X. Wu, S. K. Cheng, and S. M. Cui, Communication of Vehicle Management Unit in the Electric Vehicle, *IEEE Trans. on Magnetics*, Vol. 41, Issue 1, Part 2, Jan. 2005, pp. 514-517.
- [8] A. H. Anbuky and P. E. Pascoe, VRAL Battery State-of-Charge Estimation in Telecommunication Power Systems, *IEEE Trans. on Industrial Electronics*, Vol. 47, No. 3, Jun. 2000, pp. 565-573.
- [9] P. E. Pascoe, H. Sirisena, and A. H. Anbuky, Coup de Fouet Based VRLA Battery Capacity Estimation, *The First IEEE International Workshop on Electronic Design, Test and Applications Proceedings*, Jan. 2002, pp. 149-153.
- [10] T. Yanagihara and A. Kawamura, Residual Capacity Estimation of Sealed Lead-Acid Batteries for Electric Vehicles, *IEEE Power Engineering, Power Conversion Conference*, 1997, pp. 942-946.
- [11] M. Ceraolo and G. Pede, Techniques for Estimating the Residual Range of an Electric Vehicle, *IEEE Trans. on Vehicular Technology*, Vol. 50, Issue 1, Jan. 2001, pp. 109-115.
- [12] A. A. Thieme and B. W. Johnson, A Battery State-of-Charge Indicator for Electric Wheelchairs, *IEEE Trans. on Industrial Electronics*, Vol. 39, No. 5, Oct. 1992, pp. 398-409.
- [13] C. Y. Tseng and C. F. Lin, Estimation of the State-of-Charge of Lead Acid Batteries Used in Electric Scooters, *Journal of Power Sources*, Vol. 147, Issues 1-2, Sep. 2005, pp. 282-287.
- [14] Y. Y. Yang and T. L. Chen, Design and Implementation of Intelligent Battery Charger



and Residual Capacity Estimator for Electric Vehicles, *The 21st Symposium on Electrical Power Engineering*, Taipei, Taiwan, ROC, 2000, pp. 784-789.

- [15] S. Sato and A. Kawamura, A New Estimation Method of State of Charge Using Terminal Voltage and Internal Resistance for Lead Acid Battery, *Power Conversion Conference, PCC Osaka Proceedings*, Apr. 2002, pp. 565-570.
- [16] F. Pei, K. Zhao, Y. Luo, and X. Huang, Battery Variable Current-Discharge Resistance Characteristics and State of Charge Estimation of Electric Vehicle, *The 6th World Congress on Intelligent Control and Automation, WCICA 2006*, Vol. 2, Jun. 2006, pp. 8314-8318.
- [17] C. Barry and P. Ken, Saturation Influences on the Performance of Valve-Regulated Lead Acid Batteries, *Journal of Power Sources*, Vol. 144, Issue 2, Jun. 2005, pp. 313-321.
- [18] O. Caumont, P. L. Moigne, C. Rombaut, X. Muneret, and P. Lenain, Energy Gauge for Lead-Acid Batteries in Electric Vehicles, *IEEE Trans. on Energy Conversion*, Vol. 15, Issue 3, Sep. 2000, pp. 354-360.
- [19] S. Barsali and M. Ceraolo, Dynamical Models of Lead-Acid Batteries, *IEEE Trans. on Energy Conversion*, Vol. 17, Issue 1, Mar. 2002, pp. 16-23.
- [20] A. C. Henry, F. F. Fred, and T. Francisco, Sulfation in Lead-Acid Batteries, *Journal of Power Sources*, Vol. 129, Issue 1, Apr. 2004, pp. 113-120.
- [21] D. Linden, *Handbook of Batteries*, 2<sup>nd</sup> Ed., McGraw Hill, New York, 1995.
- [22] H. Rigakis, M. Vogiatzaki, J. Chatzakis, N. Lyberakisi, and M. Manitis, Test Pattern Designing Software for Electrical Appliance Testing Platform, *The 7th WSEAS International Conference on Applied Informatics and Communications*, Aug. 2007, pp. 236-241.

Table 3 Experiment data of the discharge test

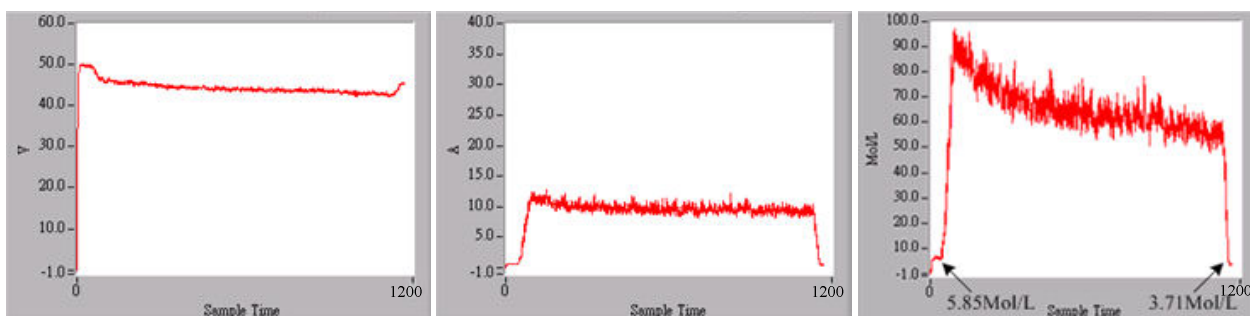
Current (A)	Discharge time (min/hour)	Battery Voltage (V)		C <sub>O</sub>	C <sub>R</sub>	SOC (%)			Error (%)	
		Primary	End			(a)	(b)	(c)	(b)-(a)	(b)-(c)
5.6	1 hour	12.80	12.05	5.96	17.86	90	89.6	78.67	0.4	10.93
5.6	46 min	12.32	10.50	4.62	15.48	56.5	57.6	62.92	1.1	5.32
11.2	10 min	12.43	11.90	4.90	16.54	65.28	64.94	93.09	0.34	28.15
11.2	10 min	12.27	11.77	4.69	15.94	54.61	54.27	86.28	0.34	32.01
11.2	10 min	12.13	11.57	4.58	15.22	45.27	44.94	79.54	0.33	34.6
11.2	10 min	12.00	11.02	4.32	13.85	36.6	36.27	72.87	0.33	36.6
11.2	5 min	11.85	10.20	4.25	13.12	26.6	26.27	69.58	0.33	43.31
16.8	10 min	12.43	11.75	4.90	16.54	65.28	64.94	89.64	0.34	24.7
16.8	10 min	12.23	11.45	4.59	15.30	51.94	51.6	79.45	0.34	27.85
16.8	10 min	12.00	9.72	4.35	14.06	36.6	36.27	69.45	0.33	33.18
16.8	3 min	11.77	9.6	4.22	13.05	22.26	20.93	66.51	1.33	45.58
22.4	10 min	12.45	11.63	4.92	16.86	66.62	66.27	86.17	0.35	19.9
22.4	10 min	12.15	10.02	4.60	15.42	46.61	46.27	72.67	0.34	26.4
22.4	4 min	11.88	9.6	4.33	13.90	28.6	28.27	67.39	0.33	39.12

Table 4 Experiment results for the constant speed driving test

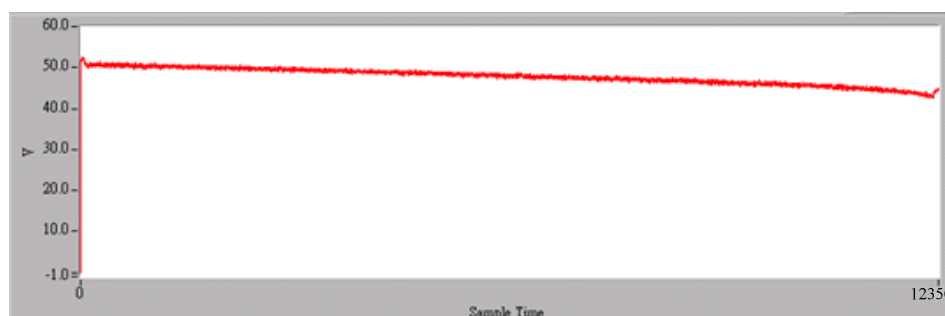
Battery	Constant speed (km/hr)	Battery voltage (V)		Driving time (sec)	C <sub>O</sub> (Mo/L)		SOC (%)	
		Primary	End		Primary	End	Primary	End
Old	15	49.75	42.9	2110.88	5.34	3.68	79.57	5
	20	50.1	42.9	1126.97	5.85	3.71	88.73	5.83
New	15	53	42.9	23161.37	6.05	3.6	100	1.66
	20	53	42.9	12337.32	6.08	3.59	100	0.83

Table 5 Experiment results for the driving mode test

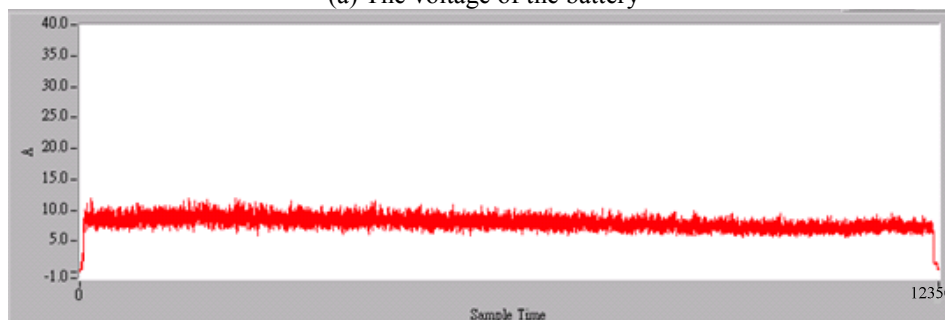
Battery	Driving mode (km/hr)	Battery voltage (V)		Driving cycle	C <sub>O</sub> (Mol/L)		SOC (%)	
		Primary	End		Primary	End	Primary	End
Old	(a)	50.05	42.9	38	5.72	3.67	94.76	4.35
New	(b)	52.3	42.9	269	6.08	3.58	100	0.2



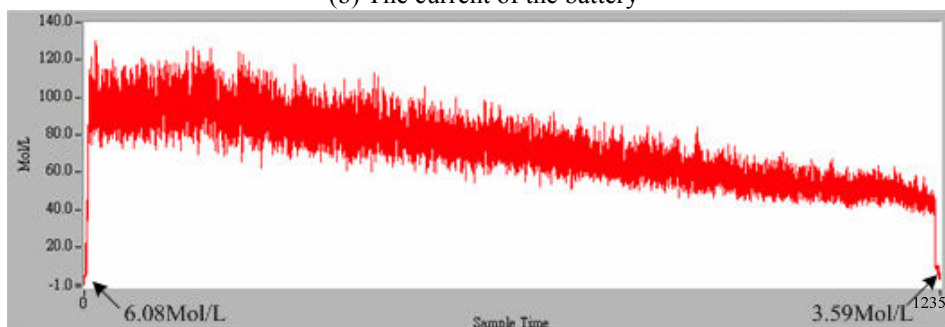
(a) The voltage of the battery (b) The current of the battery (c) The concentration of the sulfuric acid  
Fig. 5 Experiment results of the old battery for the constant speed driving test of 20 km/hr



(a) The voltage of the battery

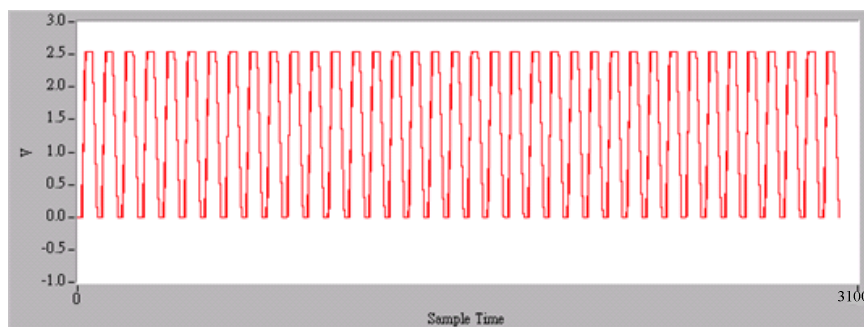


(b) The current of the battery

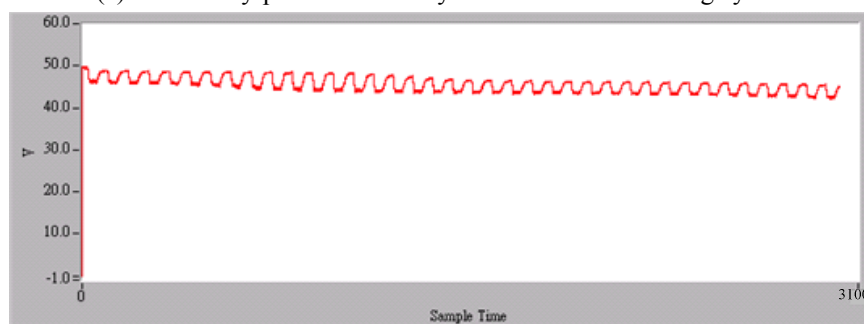


(c) The concentration of the sulfuric acid

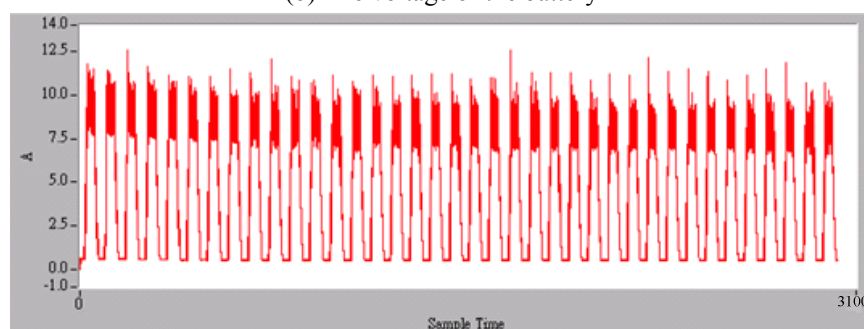
Fig. 6 Experiment results of the new battery for the constant speed driving test of 20 km/hr



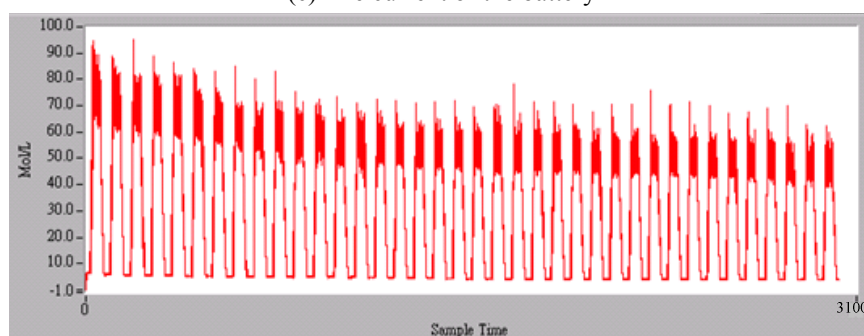
(a) The battery-powered motorcycle travels for 38 driving cycles



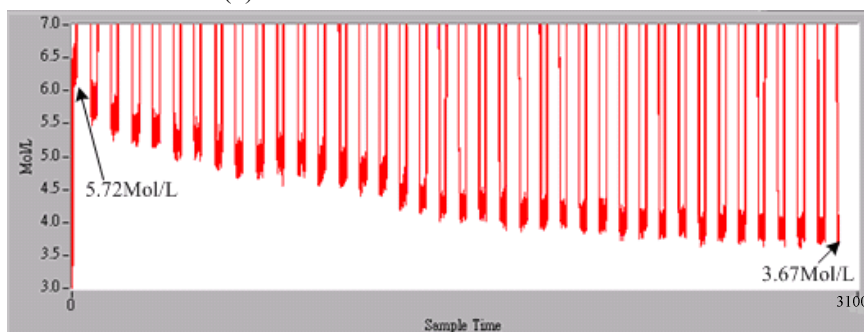
(b) The voltage of the battery



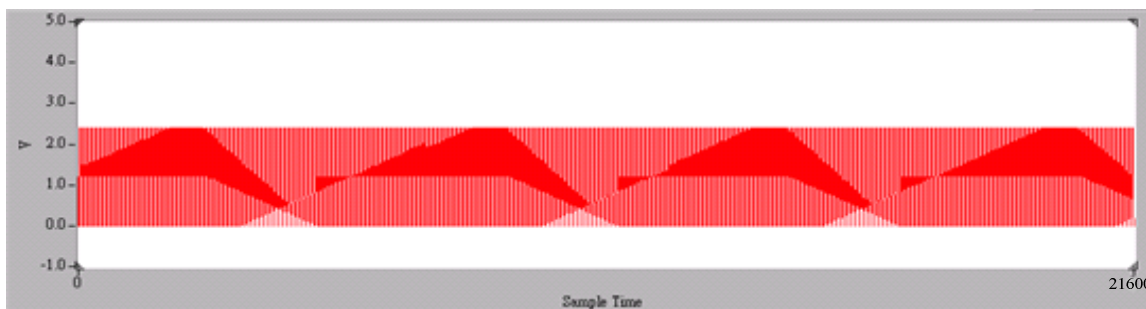
(c) The current of the battery



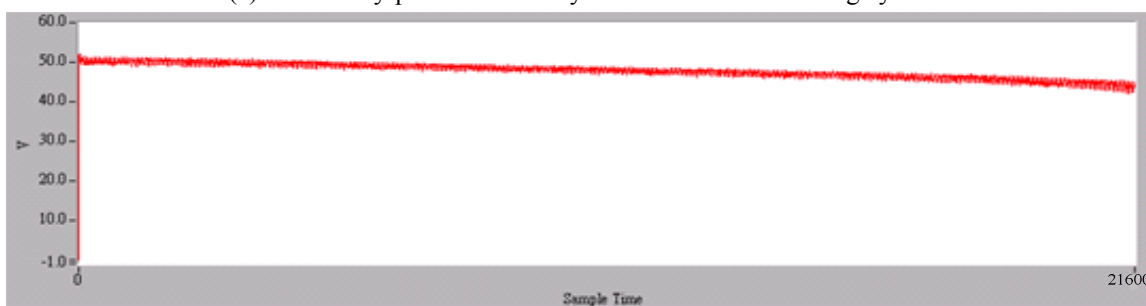
(d) The concentration of the sulfuric acid



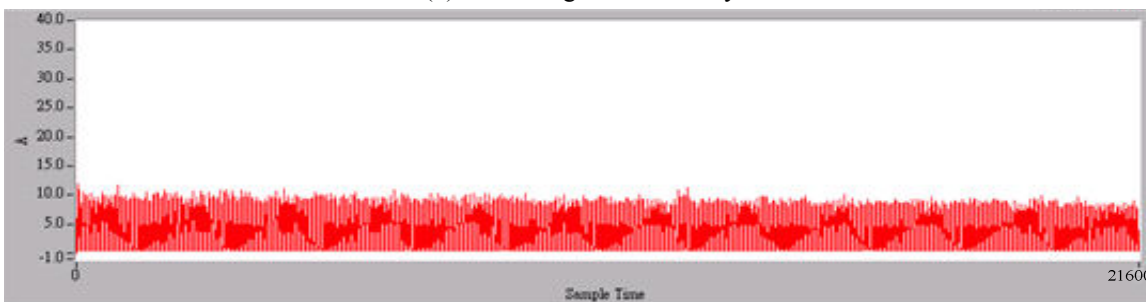
(e) The concentration of the sulfuric acid plotted with the y-axis being scaled up  
Fig. 7 Experiment results of the old battery for the driving mode test.



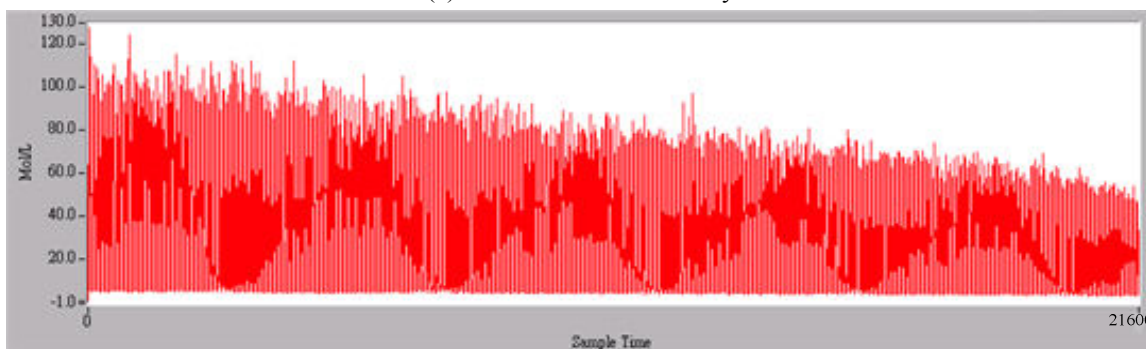
(a) The battery-powered motorcycle travels for 269 driving cycles



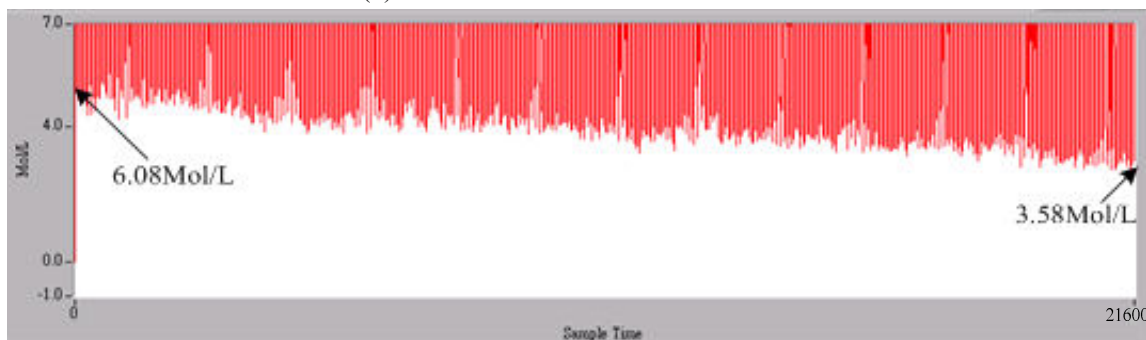
(b) The voltage of the battery



(c) The current of the battery



(d) The concentration of the sulfuric acid



(e) The concentration of the sulfuric acid plotted with the y-axis being scaled up  
Fig. 8 Experiment results of the new battery for the driving mode test